Effects of narrow-band pulse shaping on a resonant multilevel system

A. S. Meijer, A. V. Kimel, Th. Rasing, and W. J. van der Zande*
Institute of Molecules and Materials, University Nijmegen, P.O. Box 9010, NL-6500 GL Nijmegen, The Netherlands
(Received 3 July 2008; published 7 November 2008)

Phase and amplitude modulation of small frequency ranges within broadband femtosecond pulses reshape these pulses providing transients before, before and after, or after the main femtosecond pulse. The absorbed or phase-modulated frequencies appear as transients. We present experimental observations and calculations showing to what extent these transients can be used to drive population changes in the three-level 5*s*-5*p*-5*d* rubidium system in the perturbative limit. We also show computationally that these transients can assist to create complete inversion with nearly 98% population in the upper 5*d* state of rubidium at realistic intensities.

DOI: 10.1103/PhysRevA.78.053403 PACS number(s): 32.80.Qk, 32.80.Wr, 42.65.Re

I. INTRODUCTION

Steering atomic, intramolecular, and even reactive processes by manipulating coherently quantum states using light as a reagent is a long-time ambition in physics and chemistry. Coherent control employs modifying the frequency components within ultrafast pulses. Experimentally, one can change the amplitude, phase, and/or polarization of individual frequency components, changing the temporal profile of the pulses. Coherent control has been demonstrated to affect excitation processes significantly in a range of applications [1–3].

Early experimentalists applied chirp to ultrafast pulses. The pulses lengthen, while at the same time the frequency can be swept within picoseconds from red to blue or from blue to red. In simple three-level systems, such as the one studied in this paper, it was shown experimentally that 100% population transfer to the final state is possible. As an example of the often nonintuitive behavior, a "wrong" chirp, where the change in frequency does not follow the level spacings, is also able to give 100% transfer [4]. Thanks to the advent of programmable spatial light modulators (SLM), nearly arbitrary pulse shapes can be synthesized [5–9]. Whereas in simple systems, one can often predict the consequences of pulse shaping, genetic or evolutionary algorithms are used to generate the best amplitude, phase, and/or polarization distribution in order to achieve a preset goal in complex systems [3,10–16].

Also upon propagation through an absorbing gas, ultrafast pulses change shape. Semimonochromatic transient electric fields appear behind the main pulse. The resulting pulse is also called a "0π" pulse. When these pulses interact with the same gas, no overall excitation takes place as has been shown theoretically [17] and experimentally [18–21]. Of course, excitation and deexcitation processes occur when such shaped pulses interact with the gas, as has been shown experimentally by Dudovich *et al.* [22]. Beyond the perturbative regime, pulses reshaped by absorption can give nonintuitive outcomes. For example, Gürtler and van der Zande [23] reshaped far-infrared terahertz pulses using absorption by water vapor. Although in the photon picture, the photons needed to drive transitions in highly excited rubidium atoms were absent, the thus shaped pulses were found to enhance the excitation rate instead.

In this paper, we show that modulation of ultrashort pulses through narrow-band absorption excites and depletes selectively states in a multilevel system [see Fig. 1(a)] often in a nonintuitive manner. We use a programmable SLM to simulate the linear combination of a frequency-dependent phase and amplitude associated with absorption processes. This way, one can study separately the effects of power absorption and dispersion. We present calculations both in the perturbative regime and in the nonperturbative regime, showing the dependence of the coherent excitation on the semimonochromatic transients. Near 100% population in the upper 5*d* state of rubidium can be achieved in a robust way.

II. EXPERIMENT

The frequency-resolved influence of reshaped femtosecond pulses by absorption is studied in the three-level system

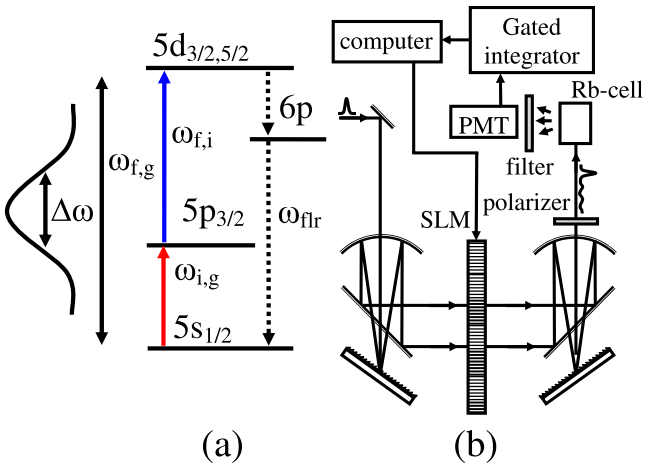

FIG. 1. (Color online) (a) Energy levels in atomic rubidium for the two-photon transitions $5s \rightarrow 5d$. The excited atoms spontaneously decay to the ground state, emitting $\omega_{flr} \approx 420$ nm photons. (b) The experimental setup consists of a pulse shaper in $4f$ geometry with a programmable SLM located in the Fourier plane. A polarizer is used, since amplitude modulation by the SLM is performed by a polarization retardation. The influence of the modulated femtosecond pulses is monitored with a PMT.

*w.vanderzande@science.ru.nl

 ©2008 The American Physical Society

of atomic rubidium; see Fig. 1(a). The resonant transitions, $5s \rightarrow 5p$ and $5p \rightarrow 5d$, correspond with transition wavelengths of $\lambda_{i,g}=780.2$ nm and $\lambda_{f,i}=776.2$ nm. A Spectra Physics 1 kHz regeneratively amplified Ti:sapphire femtosecond laser system provides 100 fs pulses of 600 μJ. The central wavelength is tuned to $\lambda_c=778.2$ nm ($\omega_c=\omega_{f,g}/2$) and the bandwidth encompasses the two transition wavelengths. After passing through a pulse shaper, the beam is sent into a 20 mm cell at room temperature containing atomic rubidium vapor. The pulse shaper is constructed in a $4f$ geometry, see Fig. 1(b), following Präkelt *et al.* [24]. The pulse shaper is aligned for zero dispersion and a polarizer before the Rb cell selects only the horizontal plane, since amplitude modulation by the SLM is performed by polarization retardation. The gratings have 1200 grooves/mm and we use 300 mm cylindrical mirrors. The active elements are arranged in a combination of two 320-pixel liquid-crystal spatial light modulators (Jenoptik, Laser Optik system GmbH, SLM-S320d). Amplitude and phase modulation can be applied independently. The pulse shaper consists of gratings and the SLM is located in the Fourier plane of the grating spectrometer. The active area of the SLM is 20 $\times$20 mm and each pixel is 100 μm wide. The frequency width of each pixel equals 126 GHz. Phase and amplitude profiles are programmed in the SLM in the form of Lorentzian absorption lines. The adjustable parameters are the position ω_0, the linewidth γ, and the strength, $\alpha_0 l$ of the absorption line. The position of the line, ω_0, is scanned through the spectrum of the femtosecond pulse in step sizes of one pixel. We will see transients appearing in front of the main pulse in the case of applying an amplitude and phase modulation. These transients seem to appear at "negative" times. However, a pulse shaper has a time window Δt, which is inversely proportional to the resolving power of the pulse shaper and is approximately 8 ps in our setup [5]. Centered around the arrival time of a transform-limited pulse (TL) at t_0, the temporal intensity can be displaced within the time window and a transient can appear in front of the pulse at negative time. The $5d$ population in Rb is quantified by measuring the fluorescence at $\approx$422 nm, due to spontaneous decay to the ground state via the $6p$ level. A photomultiplier tube (PMT) equipped with a narrow-band filter is attached to a gated integrator and computer for recording and storage. The collected signal reflects the response over the entire beam profile.

III. THEORY

A. Three-level system

Population transfer in the three-level system occurs whenever the sum of each photon pair within the pulse frequency distribution equals the energy difference between the ground and final state. The final-state amplitude $a_f^{(2)}$ is given in a perturbative picture by [25]

$$a_f^{(2)} \approx -\frac{1}{i\hbar^2}\mu_{f,i}\mu_{i,g}\left[i\pi\tilde{E}(\omega_{i,g})\tilde{E}(\omega_{f,g}-\omega_{i,g}) + \mathrm{P}\int_{-\infty}^{\infty}\frac{\tilde{E}(\omega)\tilde{E}(\omega_{f,g}-\omega)}{\omega-\omega_{i,g}}d\omega\right], \quad (1)$$

where g, i, and f label the ground, intermediate, and final states. P is the principal value of Cauchy. $\omega_{i,g}$ and $\omega_{f,i}=\omega_{f,g}-\omega_{i,g}$ are the resonant $5s \rightarrow 5p$ and $5p \rightarrow 5d$ transition frequencies. $\tilde{E}(\omega)$ is the Fourier transform of the electric field. Pulse shaping will be most effective around the two resonant transitions. The off-resonant contribution is inversely proportional to the detuning from resonance $\omega-\omega_{i,g}$, while the resonant contribution depends solely on $\tilde{E}(\omega_{i,g})$ and $\tilde{E}(\omega_{f,i})$.

From Eq. (1), Dudovich *et al.* [25] realized that the off-resonant two-photon absorption (TPA) amplitude can be enhanced significantly using a $\pi/2$ step phase mask at frequencies between the two resonances to ensure that the integrant is positive for all ω. They showed that the TPA process in the three-level rubidium atom could be enhanced by a factor of 7. The same mask, positioned elsewhere in the frequency spectrum of the pulses, could turn off the TPA process completely.

The dynamics of the three-level system excited by coherent radiation from a laser follows from the Schrödinger equation. The time evolution of the state probabilities $P_n(t)=|C_n(t)|^2$ is described by the interaction Hamiltonian and reads

$$i\hbar\begin{pmatrix}\dot{C}_g(t)\\ \dot{C}_i(t)\\ \dot{C}_f(t)\end{pmatrix}=\begin{pmatrix}0 & \Omega_{i,g}(t) & 0\\ \Omega_{g,i}(t) & \Delta_{i,g} & \Omega_{f,i}(t)\\ 0 & \Omega_{i,f}(t) & \Delta_{f,i}\end{pmatrix}\begin{pmatrix}C_g(t)\\ C_i(t)\\ C_f(t)\end{pmatrix}. \quad (2)$$

$\Delta_{i,g}=|\omega_{i,g}-\omega_c|$ is the difference between the carrier frequency and the first excitation energy. $\Delta_{f,i}=|\omega_{f,g}-2\omega_c|=0$, as the carrier frequency ω_c is resonant with the two-photon energy in our experiment. The rotating-wave approximation (RWA) has been applied. The strength of the interaction in Eq. (2) is given by the Rabi frequency $\Omega_{n,m}(t)=\varepsilon_0(t)\mu_{n,m}/2\hbar$, with $\mu_{n,m}$ the transition dipole moments and $\varepsilon_0(t)$ the temporal envelope of the femtosecond pulse. The electric field $\varepsilon(t)$ of the whole pulse is given by

$$\varepsilon(t)=\varepsilon_0(t)\cos(\omega_c t). \quad (3)$$

We use 100 fs Gaussian shaped pulses with a carrier frequency of $\omega_c=\omega_{f,g}/2$, corresponding to $\lambda_c=778.2$ nm. The transition wavelengths are $\lambda_{i,g}=780.2$ nm and $\lambda_{f,i}=776.2$ nm with transition dipole moments $\mu_{i,g}=5.87$ atomic units (a.u.) and $\mu_{f,i}=1.77$ a.u. We are mostly interested in the excited $5d$ final-state population, $P\equiv|C_f(\infty)|^2$, long after the pulse. Time-dependent results provide insight into the dynamics of the process, also in the weak field limit where Eq. (1) is valid. In the following, we present solutions using both the perturbative asymptotic solution of Eq. (1) as well as the asymptotic time-dependent solutions of Eq. (2) with $\Omega_{i,g}=10^8$ rad/s.

B. Pulse propagation

Absorption of a narrow range of frequencies involves a combination of an amplitude and phase function, as follows from the Kramers-Kronig dispersion relation, which defines the complex susceptibility $\chi(\omega)$,

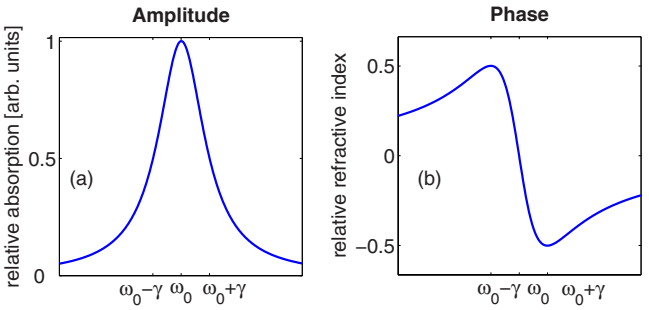

FIG. 2. (Color online) (a) The relative absorption and (b) relative refractive index of the frequency-dependent complex refractive index $\eta(\omega)$ using Eqs. (8) and (9).

$$\chi(\omega) = (N_i - N_f)\frac{e^2}{2\varepsilon_0 m\omega_0}\frac{1}{\omega - \omega_0 - i\gamma}, \tag{4}$$

where N_i and N_f are the amount of atoms in the initial and final state before excitation. ε_0, m, ω_0, and γ are the permittivity of vacuum, the electron mass, the central absorption frequency, and the half-width at half-maximum (HWHM) of the Lorentzian absorption line, respectively.

From the complex susceptibility $\chi(\omega)$ follows the complex refractive index as

$$\eta(\omega) = \eta(\omega)' - i\kappa(\omega) = \sqrt{1 + \chi(\omega)}, \tag{5}$$

with $\eta(\omega)'$ the refractive index and $\kappa(\omega)$ related to the extinction coefficient α by

$$\alpha(\omega) = \frac{\omega}{c}\kappa(\omega). \tag{6}$$

Figure 2 depicts both components of the complex refractive index using Eq. (4). A propagating plane wave affected by absorption can thus be written as

$$\tilde{E}(\omega, l) = \tilde{E}(\omega)e^{-\alpha(\omega)l}e^{-i[\eta(\omega)'-1]\omega l/c}, \tag{7}$$

where l is the propagation length through the absorbing medium and c is the speed of light. We write the absorption and dispersion profiles as

$$\alpha(\omega) = \alpha_0\frac{\gamma^2}{\gamma^2 + (\omega_0 - \omega)^2} \tag{8}$$

and

$$[\eta(\omega)'\omega - 1]/c = \alpha_0\frac{\gamma(\omega_0 - \omega)}{\gamma^2 + (\omega_0 - \omega)^2}, \tag{9}$$

where α_0 determines the strength of the interaction. With an SLM, amplitude and phase functions can be applied separately. The Fourier transform of $\tilde{E}(\omega, l)$ gives the time-dependent electric field envelope $\varepsilon_0(t)$; see Fig. 3. A first observation shows that semimonochromatic transient electric fields arise around the main pulse. Absorption $[\eta(\omega)]$ [Fig. 3(c)] has a post-transient, which is out-of-phase with the main pulse. Amplitude $[\kappa(\omega)]$ or dispersion $[\eta(\omega)']$ also give pretransients [Figs. 3(a) and 3(b)]. Amplitude modulation results in a symmetric pulse profile with transient electric fields being out-of-phase with the main pulse, while phase modulation gives an asymmetric pulse profile with a phase-matched pretransient and an out-of-phase post-transient. The transient electric fields have a duration τ $(1/e^2)$ with

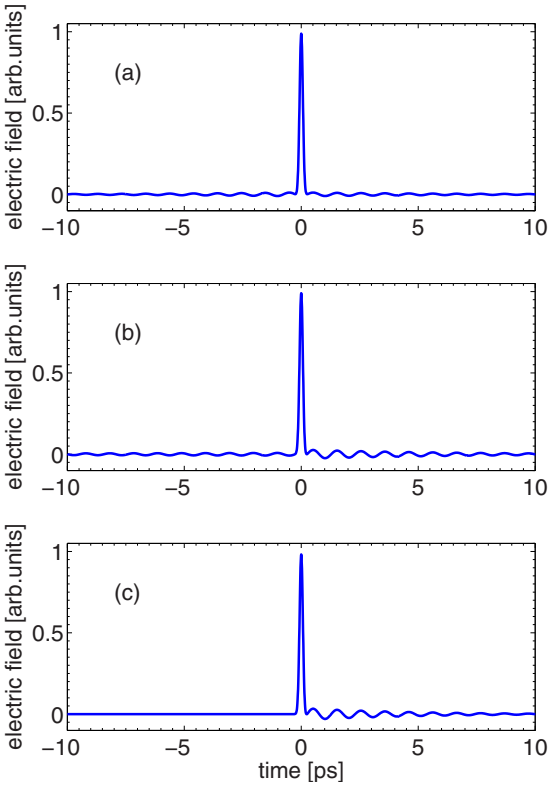

FIG. 3. (Color online) Electric fields $\varepsilon(t)$ of shaped femtosecond pulses by the Kramers-Kronig dispersion functions [Eq. (5)], $\gamma = 100$ GHz, $\alpha_0 l = 2.3$. (a) Amplitude-only, (b) phase-only, and (c) absorption-modulated pulses. Semimonochromatic transients arise around the main pulse with ≈ 5 ps decay time [Eq. (10)]. Their carrier frequencies equal the frequency $|\omega_c - \omega_0|$.

$$\tau = \frac{1}{2}\gamma^{-1}. \tag{10}$$

In all cases, the main pulse structure remains nearly the same with a slightly reduced electric field strength. Although *a priori* not obvious, the sum of amplitude [Fig. 3(a)] and phase modulation [Fig. 3(b)] closely resembles the result of reshaping using absorption [Fig. 3(c)]. In the remainder of the paper, we assume no decoherence effects due to collisions or Doppler broadening and the absorption profile is purely Lorentzian. The pixel width in our spatial light modulators forces us to use linewidths that are larger than atomic absorption lines in gases.

IV. RESULTS AND DISCUSSION

We investigate the influence of shaped femtosecond pulses by narrow-band amplitude [Fig. 3(a)], phase [Fig. 3(b)], and absorption [Fig. 3(c)] modulation on the two-photon excitation in the three-level atomic system of ru-

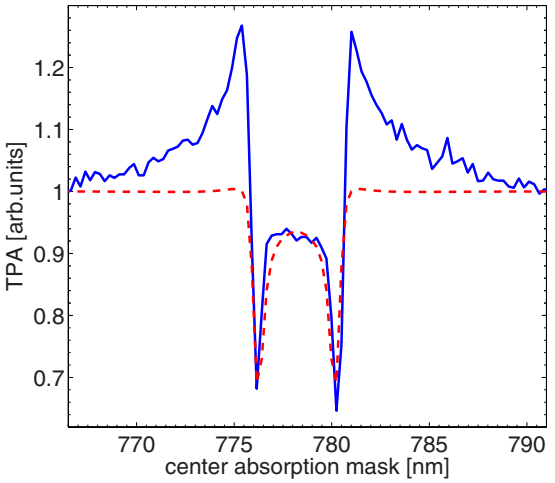

FIG. 4. (Color online) The experimental (solid) and the simulated (dashed) frequency resolved TPA signal for amplitude-modulated femtosecond pulses according to the Kramers-Kronig dispersion function (γ=100 GHz, $\alpha_0 l$=2.3).

bidium. The used absorption parameters are γ=100 GHz and $\alpha_0 l$=2.3, implying an extinction of 90% at the central frequency ω_0.

We accompany measurements of the 5*d*-state population with calculations both time-dependent and time-independent. The time-independent calculations Eq. (1) include the discretization of the modulation mask. In the remainder of this paper, we will focus on the final 5*d*-state population $|C_f(t)|^2$. We discuss the time evolution during the whole pulse for the two important line positions $\omega_0=\omega_{i,g}$ and $\omega_0=\omega_{f,i}$.

In Fig. 4, the experimental (solid) and calculated (dashed) TPA signal are shown as a function of the central position of the amplitude function [Fig. 2(a)]. A transform-limited (TL) pulse gives a TPA signal of 1. The experimental results reveal a significant enhancement around the two discrete resonances and a significant reduction at the resonances. Only the latter is reproduced by the simulations. The reduction reflects the intuitive picture that both resonant photons are needed in the TPA process. The discrete nature of the modulation does not have a large effect on the results of the simulations. We will return to the discrepancies between our model calculations and the experimental result below.

In Fig. 5, we present the time evolution of the 5*d*-state population in the TPA process for an amplitude-modulated femtosecond pulse for two positions of ω_0. With the absorption feature at $\omega_0=\omega_{i,g}$, one observes a single step in the population due to the femtosecond pulse. The small oscillations reflect the nonresonant excitation at $\omega=\omega_{f,i}$ by the post-transient. The pretransient only excites 5*p* state population (inset in Fig. 5) and a quadratic increase is observed before the main pulse. In accord with the π shift of the pretransient, the intense main pulse initially depletes the 5*p* state. This initial small reduction of the 5*p*-state population is the reason for the small TPA signal. With the mask at $\omega_0=\omega_{f,i}$, one observes that the post-transient in spite of its small energy content reduces the final-state population by almost a factor of 2. This resembles a pump-dump sequence, in which the transient acts as dump. The important observation is that

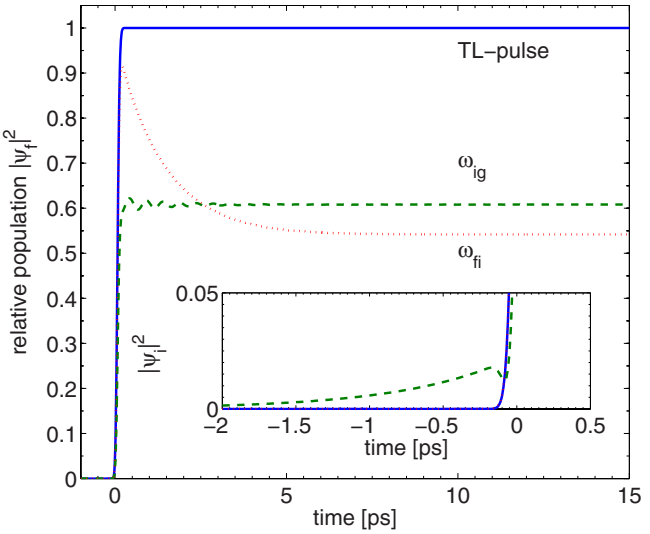

FIG. 5. (Color online) The time evolution of the 5*d*-state population, $|\psi_f|^2$, for TL pulses (solid) and amplitude-modulated femtosecond pulses (γ=100 GHz, $\alpha_0 l$=2.3) with central mask positions $\omega_0=\omega_{i,g}$ (dashed) and $\omega_0=\omega_{f,i}$ (dotted). The inset shows the time evolution of the 5*p*-state population $|\psi_i|^2$.

because of the coherent nature, weak transients influence final populations significantly.

Figure 6 shows the spectrally resolved TPA signal for a modulated pulse by the phase function [Fig. 2(b)]. Nonintuitively, we observe a sharp increase in the TPA signal with the mask at the 5*s*-5*p* resonance. The increase equals 115% at $\lambda_{i,g}$ and the decrease equals 45% at $\lambda_{f,i}$. The experimental result is well reproduced, although also here the coherent effects seem to be larger than calculated around $\lambda_{i,g}$ and $\lambda_{f,i}$.

The time evolution of the final-state population $|C_f|^2$ in Fig. 7 illustrates the cause of the enhanced population transfer in comparison with a TL pulse. The phase-matched pretransient at $\omega_{i,g}$ (dashed) will transfer population to the intermediate 5*p* state, which will be enhanced further by the main

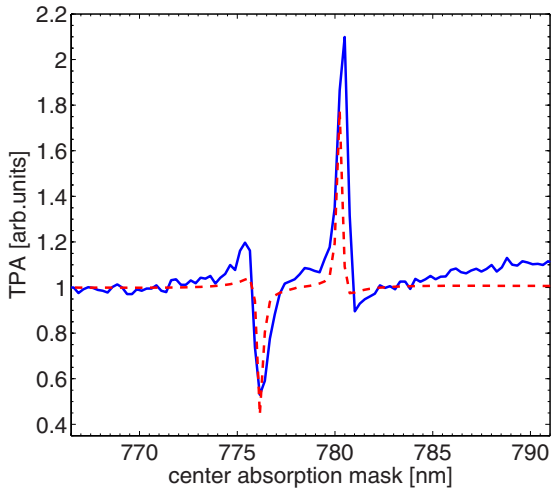

FIG. 6. (Color online) The experimental (solid) and the simulated (dashed) frequency-resolved TPA signal for phase-modulated femtosecond pulses according to the Kramers-Kronig dispersion function (γ=100 GHz, $\alpha_0 l$=2.3).

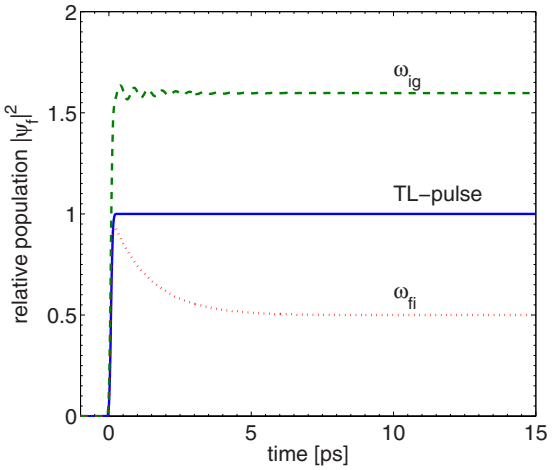

FIG. 7. (Color online) The time evolution of the $5d$-state population, $|\psi_f|^2$, for a TL pulse (solid) and a phase-modulated femtosecond pulse (γ=100 GHz, α_0=2.3) with central mask positions $\omega_0=\omega_{i,g}$ (dashed) and $\omega_0=\omega_{f,i}$ (dotted).

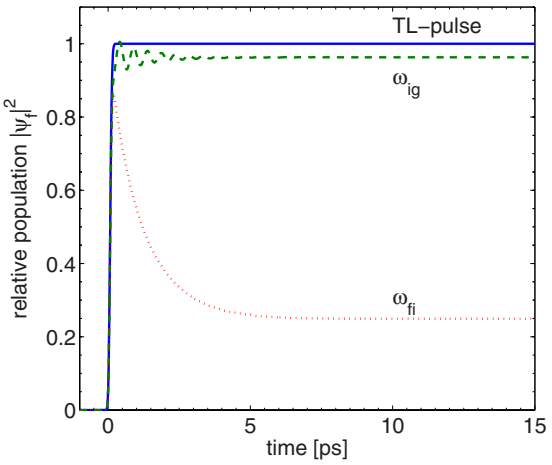

FIG. 9. (Color online) The time evolution of the $5d$-state population, $|\psi_f|^2$, for a TL pulse and an absorption-modulated femtosecond pulse (γ=100 GHz, α_0=2.3) with central mask positions $\omega_0=\omega_{i,g}$ (dashed) and $\omega_0=\omega_{f,i}$ (dotted).

pulse. The out-of-phase post-transient can be largely ignored since it only connects the ground and intermediate states. A phase modulation of the femtosecond pulse at $\omega_{f,i}$ (dotted) also creates a pretransient, which has no effect as no population is present in the intermediate state. Whereas the main pulse redistributes almost as much population to the final state as a TL pulse, the π-shifted post-transient deexcites the final state.

Finally, we will consider the situation that resembles narrow-band absorption [Eq. (4)]. Figure 8 shows the spectrally resolved influence of an absorption-modulated femtosecond pulse on the final-state population. Again, large effects are observed only around the transition frequencies $\omega_{f,i}$ and $\omega_{f,i}$.

In agreement with the previous results, around the resonances the TPA signal reacts more strongly on the pulse

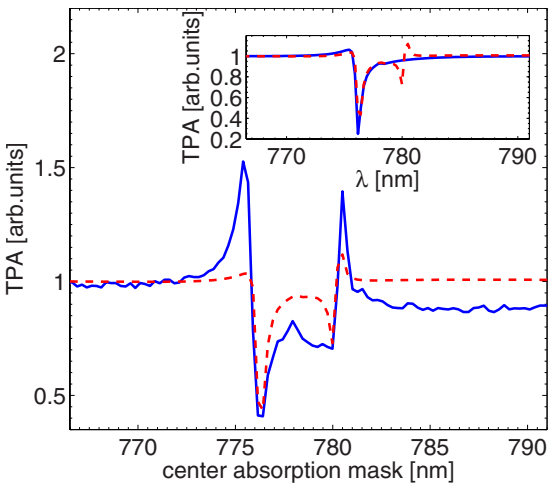

FIG. 8. (Color online) The experimental (solid) and the simulated (dashed) frequency-resolved TPA signal for absorption-modulated femtosecond pulses according to the Kramers-Kronig dispersion functions (γ=100 GHz, $\alpha_0 l$=2.3). The inset shows the effect of the discretization (dashed) on an ideal continuous modulation (solid).

shaping than the calculations predict. Also in between the two resonances, the experiment is more sensitive to changes than the calculations. However, qualitatively, the simulation resembles our observations closely. In this case, the inset depicts that the discrete nature of the phase and amplitude function has an effect, and that the TPA is nearly unchanged when absorbing $\omega_{i,g}$. The observations can be well understood in the pump-dump picture. The time evolution of the $5d$ state shows in Fig. 9 that in the absence of a pretransient, the femtosecond pulse excites nearly the same amount of population to the $5d$ state when absorbing $\omega_{i,g}$. The observations can be well understood in the pump-dump picture. With the mask at $\omega_{f,i}$, the small energy of the out-of-phase post-transient depletes the $5d$ state. When $\omega_0=\omega_{i,g}$, the post-transition does not change the final-state population and for an observer the fluorescence intensity remains unchanged

As mentioned before, amplitude modulation and phase modulation are approximately additive when looking at the resulting time-dependent pulses in Fig. 3. In this study, we also found that the TPA signals in the three different situations are connected in a simple but highly nonintuitive manner. Comparing Figs. 4, 6, and 8, one can appreciate that the following equality holds:

$$P_f(\text{amplitude})P_f(\text{phase}) \approx P_f(\text{absorption})P_f(\text{TL}). \quad (11)$$

Figure 10 shows the equality in the case of the calculations as well as the agreement when using the experimental data. We checked that this is not true on the level of amplitudes: $a_f^{\text{amp}}a_f^{\text{ph}} \neq a_f^{\text{abs}}a_f^{\text{TL}}$. The fact that the experimental data obey this equality, as depicted in Fig. 10(a), shows the consistency of our experimental observations.

We conclude that the two 320-pixel spatial light modulators have small extra effects that are not correctly modeled by taking step functions when going from pixel to pixel. With ultrafast pulses, chirp in a pulse cannot always be prevented due to dispersion in many optical components. Numerically, we have looked at the effect of chirp on the TPA signal. We found that up to a pulse elongation of a factor of

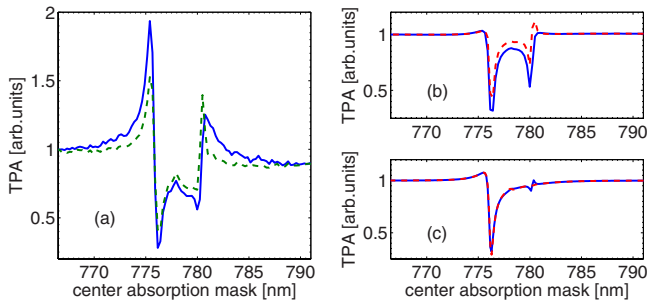

FIG. 10. (Color online) Comparison of the product of the amplitude and phase-modulated (solid) TPA signal with the absorption-modulated (dashed) TPA signal [Eq. (11)]. (a) Experiment, (b) simulation with discretization, and (c) simulation without discretization.

10, the effects on the form of the response on moving an amplitude profile through the spectrum are small. The absolute signal decreases significantly. Hence, we rule out (linear) chirp as an explanation of the difference between our calculations and observations. The consistent discrepancy between the calculations and measurements (Fig. 10) can be assigned to the space-time coupling inherent in pulse shapers. Recently, Sussman *et al.* [26] have shown that spectral phase jumps have a dramatic effect on the frequency components that fall on the pixels in the mask where the phase is changing. Diffraction will change the programmed phase structure and change the far-field spectral intensity distribution. While this may be a small effect for most coherent control experiments given that it is only one frequency component among many, it is very important here since only the near-resonant frequency components are playing an important role [22], because in our experiments we apply rapid phase changes over a relatively small range of frequencies.

The above result shows that weak semimonochromatic post-transients due to absorption, resonant with a transition in the Rb three-level system, significantly reduce the TPA signal. Beyond the perturbative limit when the main pulse is sufficiently strong, saturation can occur during the main ultrafast pulse. Since saturation is accompanied with phase changes in the time-varying coefficients $C_n(t)$, an out-of phase post-transient can be suddenly phase-matched and can become an effective driving field for further coherent excitations.

We present one computational example optimizing the excitation to the final $5d$ state of rubidium using a single narrow-band amplitude modulation with intensities that are in reach of present-day amplified Ti-sapphire lasers. Figure 11 shows the time evolution of the $5d$-state population $|C_f|^2$ for the reshaped femtosecond pulse (dashed) having an optimized absorption profile at $\omega_0=\omega_{f,i}$. We adjust the linewidth and the absorption strength. As a result, the shaped femtosecond pulse enhances the TPA rate with a factor 8.8, while approximately 97% of the population is transferred to the final state while being at a Rabi frequency of only $\Omega_{i,g}$ =4.1 THz. The linewidth was taken to be 4.1 GHz, while the resonant absorption coefficient $\alpha_0 l$ is increased to 2.57. As the inset shows, within the time duration of the main pulse an oscillation, similar to half a Rabi cycle, is seen, such that

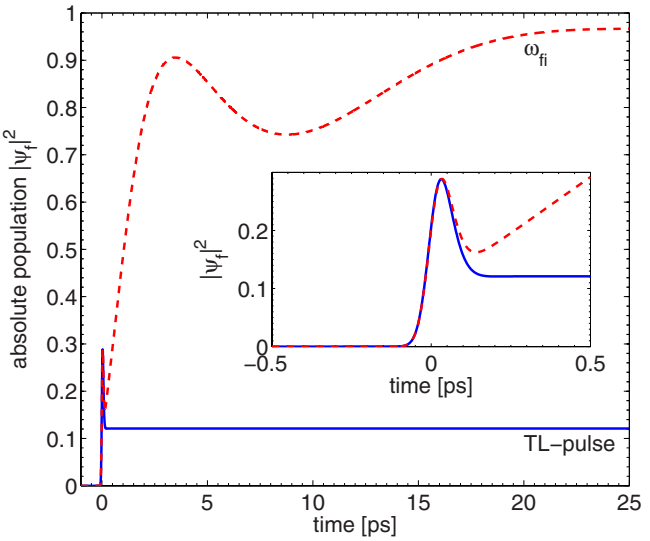

FIG. 11. (Color online) The time evolution of the $5d$ population for a TL pulse (solid) and an optimized absorption-modulated femtosecond (dashed) (γ=4.1 GHz, α_0=2.57) at a Rabi frequency of 4.1 THz. In the presence of the main pulse, half a Rabi cycle is covered and suddenly the post-transient is phase-matched with $5d$-state population. The semimonochromatic transient efficiently populates the final state with nearly complete population inversion.

the post-transient is suddenly phase-matched with the time-varying coefficient $C_f(t)$. Population is transferred to the final state in the presence of the transient electric field with nearly complete population inversion. The successful solutions not only have to increase the $5d$ population, but must prevent population trapping at the ground or intermediate state.

Clearly, semimonochromatic transients can be used to populate and depopulate excited states in multilevel systems. The reshaped pulses by narrow-band absorption have similarities with self-induced transparency, i.e., lossless propagation in normally absorbing media. The use of programmable spatial light modulators may result in multiresonance self-induced transparency. Future studies may involve searching for state-specific excitation in multiphoton processes by combining complex structures with selective narrow-band absorption. In the present research, only amplitude and phase modulation was used. Polarization modulation enables manipulation of vectorial properties. For example, Dudovich *et al.* [27] applied polarization masks in the presently used rubidium system, obtaining angular momentum control. It has also been recently demonstrated that with the help of circular polarized laser pulses, one can excite and control spin precessions in magnetically ordered materials [28] and even reverse magnetization on a subpicosecond time scale [29]. Obviously, many opportunities exist to control the coherent aspects of light in the interaction with quantized multilevel systems. This research shows a beginning of this.

V. CONCLUSIONS

We have demonstrated that absorption reshaped femtosecond pulses can manipulate two-photon absorption efficiency

in resonant three-level systems. The experimental dependency of the two-photon absorption signal on narrow-band phase and amplitude modulation is well described theoretically. Large effects occur near the resonant transition frequencies $\omega_{i,g}$ and $\omega_{f,i}$. Understanding emerges from perturbation theory, which implies quantum-mechanical interferences between resonant and off-resonant contributions. The excitation process is often better understood in a time-dependent picture. As a consequence of modulating a narrow band of frequencies within the pulse distribution, semimonochromatic transients arise around the main pulse with small intensities. Electronic state wave packets are created by the main pulse. The transient electric fields transfer population coherently back to a lower state or up to a higher-lying state. These semimonochromatic transients are ideal driving electric fields to enhance or deplete state population.

In absorption processes, amplitude and phase effects are coupled. Comparison of the absorption reshaped time structure reveals that the amplitude-only and phase-only reshaped temporal pulses are approximately additive. Also the TPA behavior in the three different situations is connected, in a rather simple but not obvious manner. The TPA of absorption is well approximated by the product of the TPA signal for amplitude only and phase only. The good experimental agreement illustrates the consistency throughout the measured TPA signals. Numerically, an optimal pulse has been designed, which takes advantage of Rabi cycling during the main pulse. For that situation, 97% of the population is transferred to the final state. Without any genetic optimization algorithm, we are able to find an absorption reshaped femtosecond pulse, which holds the ability for complete inversion. It is fascinating to observe that very weak resonant transients have such a profound effect on excitation processes, while at the same time holding a very small fraction of the total energy in the pulse. We expect that when using stronger pulses, highly nonintuitive results can be achieved such as population of single levels in a multilevel resonant excitation scheme and complete inversion between any pair of excited states in a multilevel system.

ACKNOWLEDGMENTS

The authors would like to thank Ing. A.F. van Etteger for his technical support, and M.J.J. Vrakking for his stimulating discussions and computational support. This work is supported by the "Stichting Technische Wetenschappen (STW)," which is financially supported by the "Nederlandse Organisatie voor Wetenschappelijk Onderzoek (NWO)."

[1] M. Shapiro and P. Brumer, J. Chem. Phys. **84**, 4103 (1986).
[2] D. J. Tannor and S. A. Rice, J. Chem. Phys. **83**, 5013 (1985).
[3] R. S. Judson and H. Rabitz, Phys. Rev. Lett. **68**, 1500 (1992).
[4] B. Broers, L. D. Noordam, and H. B. van Linden van den Heuvell, Phys. Rev. A **46**, 2749 (1992).
[5] A. M. Weiner, Prog. Quantum Electron. **19**, 161 (1995).
[6] C. W. Hillegas, J. X. Tull, D. Goswami, D. Strickland, and W. S. Warren, Opt. Lett. **19**, 737 (1994).
[7] D. Gowswami, Phys. Rep. **374**, 385 (2003).
[8] J. Degert, W. Wohlleben, B. Chatel, M. Motzkus, and B. Girard, Phys. Rev. Lett. **89**, 203003 (2002).
[9] C. Petersen, E. Péronne, J. Thøgersen, H. Stapelfeldt, and M. Machholm, Phys. Rev. A **70**, 033404 (2004).
[10] T. Baumert, T. Brixner, V. Seyfried, M. Strehle, and G. Gerber, Appl. Phys. B: Lasers Opt. **65**, 779 (1997).
[11] D. Meshulach and Y. Silberberg, Phys. Rev. A **60**, 1287 (1999).
[12] H. Rabitz, R. de Vivie-Riedle, M. Motzkus, and K. Kompa, Science **288**, 824 (2000).
[13] R. Bartels, S. Backus, E. Zeek, L. Misoguti, G. Vdovin, I. P. Christov, M. M. Murnane, and H. C. Kapteyn, Nature **406**, 164 (2000).
[14] J. L. Herek, W. Wohlleben, R. J. Cogdell, D. Zeidler, and M. Motzkus, Nature **417**, 533 (2002).
[15] T. Brixner, N. H. Damrauer, G. Krampert, P. Niklaus, and G. Gerber, J. Opt. Soc. Am. B **20**, 878 (2003).
[16] C. Trallero-Herrero and T. C. Weinacht, Phys. Rev. A **75**, 063401 (2007).
[17] M. D. Crisp, Phys. Rev. A **1**, 1604 (1970).
[18] S. L. McCall and E. L. Hahn, Phys. Rev. **183**, 457 (1969).
[19] J. E. Rothenberg, D. Grischkowsky, and A. C. Balant, Phys. Rev. Lett. **53**, 552 (1984).
[20] U. Kallmann, S. Brattke, and W. Hartmann, Phys. Rev. A **59**, 814 (1999).
[21] J. K. Ranka, R. W. Schirmer, and A. L. Gaeta, Phys. Rev. A **57**, R36 (1998).
[22] N. Dudovich, D. Oron, and Y. Silberberg, Phys. Rev. Lett. **88**, 123004 (2002).
[23] A. Gürtler and W. J. van der Zande, Phys. Rev. Lett. **93**, 153002 (2004).
[24] A. Präkelt, M. Wollenhaupt, A. Assion, C. Horn, C. Sarpe-Tudoran, M. Winter, and T. Baumert, Rev. Sci. Instrum. **74**, 4950 (2003).
[25] N. Dudovich, B. Dayan, S. M. GallagherFaeder, and Y. Silberberg, Phys. Rev. Lett. **86**, 47 (2001).
[26] B. J. Sussman, R. Lausten, and A. Stolow, Phys. Rev. A **77**, 043416 (2008).
[27] N. Dudovich, D. Oron, and Y. Silberberg, Phys. Rev. Lett. **92**, 103003 (2004).
[28] A. V. Kimel, A. Kirilyuk, P. A. Usachev, R. V. Pisarev, A. M. Balbashov, and T. Rasing, Nature **435**, 655 (2005).
[29] C. D. Stanciu, F. Hansteen, A. V. Kimel, A. Kirilyuk, A. Tsukamoto, A. Itoh, and T. Rasing, Phys. Rev. Lett. **99**, 047601 (2007).